

**Structure and rheology during shear-induced crystallization of a latex suspension**

P. Panine and T. Narayanan\*

*European Synchrotron Radiation Facility, F-38043 Grenoble Cedex, France*

J. Vermant and J. Mewis

*Department of Chemical Engineering, K.U. Leuven, de Croylaan 46, B-3001 Leuven, Belgium*

(Received 31 January 2002; published 28 August 2002)

Microstructure and rheology of a concentrated sterically stabilized colloidal suspension undergoing flow-induced ordering was studied by combined small-angle x-ray scattering and rheometry. This system is known to form bundlelike structures at high stress values in continuous shear flow. Under large amplitude oscillatory flow, hexagonal close-packed crystalline domains are formed within 1 sec of the inception of shear. In the intermediate range of frequencies and amplitudes, a nearly perfect hexagonally close-packed layer structure was observed after the cessation of flow. Lower frequencies or stress amplitudes resulted in polycrystals and, on the other hand, high frequencies or stress amplitudes led to partial melting of the layered structure. During the oscillatory flow, the intensity of the Bragg peaks showed pronounced oscillations.

DOI: 10.1103/PhysRevE.66.022401

PACS number(s): 82.70.Dd, 83.85.Hf, 83.60.Rs

The interplay between microstructure and rheology is a long-standing issue in colloid science [1]. One of the well-known examples is that of colloidal crystals subjected to shear flow [3,2,4]. Three-dimensional crystals can be transformed into two-dimensional layered structures and eventually to liquidlike structures at high shear rates [2,5]. This shear melting is accompanied by a dependence of the viscosity on the applied shear rate. In a colloidal fluid, the shear flow becomes dominant over the Brownian motion when the Peclet number ( $\dot{\gamma}\tau_D$ ) > 1, where  $\dot{\gamma}$  and  $\tau_D$  are the shear rate and particle diffusion time, respectively. A distortion of the static structure is expected for  $\dot{\gamma}\tau_D > 1$ . At still higher  $\dot{\gamma}$  a layered structure can arise even in a fluidlike colloidal suspension. At low shear rates, two-dimensional hexagonal close-packed layers can be formed that arrange in the flow direction and enhance the flow. The layer sliding mechanism of flow has also been studied in spherical micelles of block copolymer systems [6–9].

Understanding how the hydrodynamic forces influence the suspension structure and determine the macroscopic properties is essential in predicting the dynamic behavior of viscous suspensions [10]. The Brownian and hydrodynamic interactions among particles determine to a large extent the suspension viscosity. They depend strongly on how the flow-induced changes in the microstructure alter the interparticle distance. Distortions of a liquidlike structure or microstructural transitions will hence entail nonlinear flow curves [10,11]. In order to resolve the underlying issues, it is important to obtain microstructure and rheological parameters simultaneously. In this paper, we report the feasibility of such experiments by combining small-angle x-ray scattering (SAXS) and rheology. We have studied the shear-induced ordering of a concentrated sterically stabilized colloidal system. At high stress levels, large scale bundle structures have been observed in this system by means of small-angle light

scattering [12]. Formation of these bundles is accompanied by a decrease in viscosity. It has been suggested that these large scale structures are a result of either a shear-banding instability or the coexistence of ordered and disordered domains [13].

The initial state of our samples contained in a Couette type flow cell was disordered. Under steady shear, the disordered structure transforms gradually to an ordered crystalline phase as a function of applied stress ( $\sigma$ ) levels, as for other sterically stabilized systems [2]. In this work, we investigated the evolution of the microstructure as a function of time with the application of oscillatory shear with controlled peak stresses. The oscillatory shear flow permitted us to obtain a perfect crystalline order as envisaged by Loose and Ackerson [14]. The layered structures observed in this case resemble those observed in the case of electrostatically stabilized colloids [5].

The colloidal particles are composed of a poly(butylacrylate-styrene) core and a shell of stabilizing surfactant. Suspensions of such particles in an aqueous medium mimic a hard-sphere behavior. The sample used here is the same as that labeled  $A_1$  in an earlier small-angle light scattering study [12]. It has an effective hard-sphere volume fraction of 0.62 as determined from rheological measurements [12,15]. The particle form factor was determined by the scattering from a dilute suspension ( $\phi \sim 0.003$ ). The SAXS is dominated by the core region of the particles because of the higher electronic contrast. The measured form factor yielded an average core diameter of  $111.2 \pm 0.8$  nm.

The sample was contained in a polycarbonate Searle type Couette cell, which is coupled to a rheometer (Haake, RT-20). The outer cylinder has an inner diameter of 20 mm with a shear gap of 1 mm. The details of this apparatus are given elsewhere [16]. Prior to loading in the shear cell, the sample was vigorously stirred to destroy any residual crystalline ordering. The use of a rheometer permitted to apply stress controlled shearing motion and to obtain the rheological parameters simultaneously. The sample was subjected to oscillatory shears of small frequency  $f$  and controlled peak stresses ( $\sigma$ ).

\*Electronic address: narayan@esrf.fr

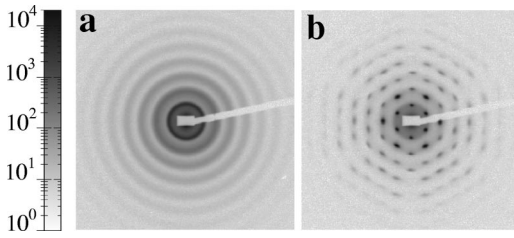


FIG. 1. SAXS patterns from a latex suspension before and after applying an oscillatory shear of  $\sigma=400$  Pa and  $f=6.8$  Hz [(a) and (b), respectively] for 25 sec. The initial suspension has a disordered glasslike structure, and a highly twinned fcc structure is developed during the oscillatory shear.

The SAXS measurements were performed at the high brilliance beam line (ID2) at the European Synchrotron Radiation Facility in Grenoble, France. The pinhole camera setup and the standard procedure for data acquisition and treatment are described elsewhere [17]. The beam size at the sample position was about  $0.1 \text{ mm} \times 0.1 \text{ mm}$ . The two-dimensional (2D) SAXS patterns were acquired using an image intensified charge-coupled device (CCD) detector. The incident wavelength  $\lambda$  was  $0.099 \text{ nm}$  and a sample-to-detector distance of  $10 \text{ m}$  was used. This combination provided a useful scattering wave vector ( $q$ ) range of  $0.02 \text{ nm}^{-1} \leq q \leq 1 \text{ nm}^{-1}$ . Here  $q$  is given by  $(4\pi/\lambda) \sin(\theta/2)$ , with  $\theta$  being the scattering angle.

The time evolution of the structure was monitored from the initiation of oscillatory shear. The data acquisition is synchronized with the onset of oscillation and typically five frames were acquired per second and up to 120 frames were recorded in a given experiment. The measurements were repeated for different frequencies (1–10 Hz) and  $\sigma$  values (100–1000 Pa). Further images were acquired after the cessation of shear flow to determine the equilibrium structure. Most of the measurements were taken with the beam passing along the velocity gradient ( $\vec{\nabla} \vec{v}$ ) direction through the center of the shear cell. Additional measurements were also made along the velocity direction ( $\vec{v}$ ) with the beam passing through the center of the gap. The images were subsequently normalized for the detector response, incident flux, exposure time, and sample transmission [17]. The normalized background of the Couette cell was subtracted from each intensity pattern.

The powder averaged static structure factor  $S(q)$  of the initial suspension indicated that the structure is disordered with particles closely packed. Figure 1(a) shows the typical 2-d SAXS pattern from this suspension. The height of the first maxima of  $S(q)$  is about 3.3 which is above the static criterion for the liquid state (2.85) [18]. The concentric rings in the initial static scattering pattern ( $\sigma=0$ ) shows the  $S(q)$  of the disordered structure modulated by the particle form factor. Figure 1(b) shows the change in the scattering pattern upon the cessation of an oscillatory shear of  $\sigma$  of 400 Pa at a frequency of 6.8 Hz for 25 sec. The appearance of the hexagonally close-packed (hcp) layer structure is directly evident. When these layers slip past each other under an oscil-

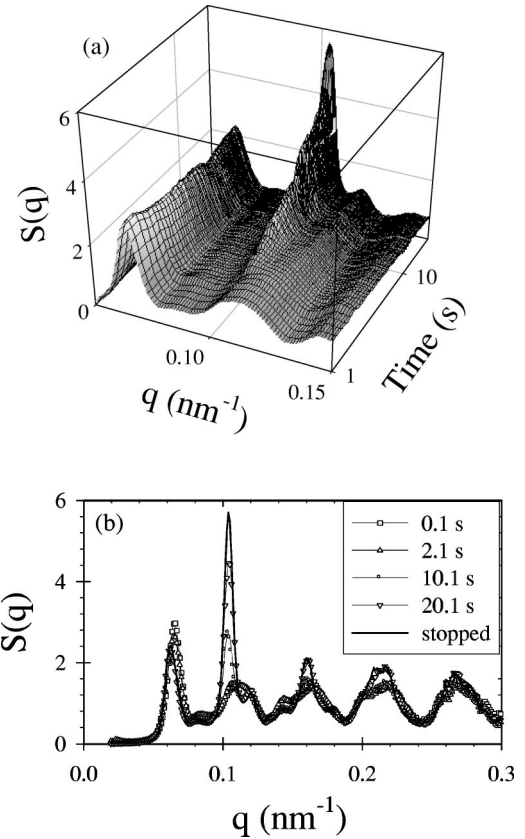


FIG. 2. (a) Time evolution of azimuthally averaged  $S(q)$  of the latex suspension for an oscillatory shear of  $\sigma=400$  Pa and  $f=6.8$  Hz. For the sake of clarity, only the inner diffraction peaks are shown. (b)  $S(q)$  at selected intervals of time. The peak positions can be indexed as  $1:\sqrt{3}:2:\sqrt{7}:3:\sqrt{12}:\dots$ . The artificial peaks around  $q=0.081 \text{ nm}^{-1}$  and  $0.142 \text{ nm}^{-1}$  are artifacts of form factor division.

latory shear of optimum  $\sigma$  and  $f$ , the stacking faults are gradually annealed resulting in a perfect periodic structure [7,14].

In order to analyze the time evolution of the structure during the initial stages of oscillatory shear, we reduced the azimuthally averaged scattered intensity to  $S(q)$  by dividing by the experimentally measured particle form factor. Figure 2(a) shows the time evolution of  $S(q)$  in the  $\vec{v}-(\vec{\nabla} \times \vec{v})$  plane for an oscillatory shear of  $\sigma=400$  Pa and  $f=6.8$  Hz. The onset of crystallization within 1 sec is marked by the appearance of the crystalline peaks. The first-order correlation peak of the initial disordered system at  $q \sim 0.065 \text{ nm}^{-1}$  vanishes after about 10 sec signifying the complete transformation of the sample to a layered crystalline form. This structure under static conditions remains stable for a long time (at least several hours). Figure 2(b) depicts the  $S(q)$  at selected intervals of time. The crystalline peaks appear at  $q$ 's ( $\text{nm}^{-1}$ );  $0.0617, 0.104, 0.12, 0.16, 0.18, 0.209, 0.218, \dots$ . The observed first peak at  $0.0617$  corresponds to a lattice constant  $d$  of  $117.5 \text{ nm}$  ( $4\pi/\sqrt{3}d$ ) and it is consistent with the known size and packing fraction of the particles.

The SAXS pattern in Fig. 1(b) compares well with the model calculations of Loose and Ackerson [14]. These mod-

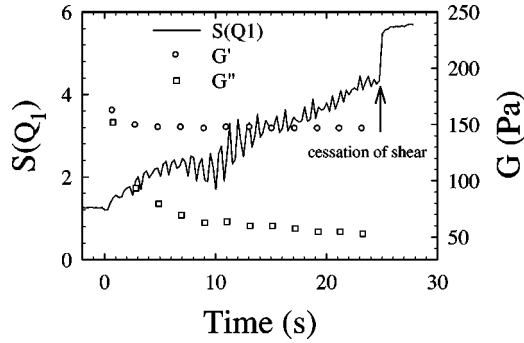


FIG. 3. Time evolution of the shear moduli ( $G'$  and  $G''$ ) and crystallinity as determined by the height of the first-order fcc peak at  $q \sim 0.104 \text{ nm}^{-1}$ ,  $S(Q_1)$ , for an oscillatory shear of  $\sigma = 400 \text{ Pa}$  and  $f = 6.8 \text{ Hz}$ . Both  $G''$  and  $S(Q_1)$  evolved in tandem and the crystallinity increased upon the cessation of shear.

els predict the diffraction patterns corresponding to different scenarios in hcp layered structures undergoing shear flow. Here the layered planes are parallel to the velocity direction ( $\vec{v}$ ). There is an exact match between Fig. 1(b) and the predicted structure factor for a highly twinned face centered cubic (fcc) structure [14]. For any given order of diffraction, there is no detectable variation in the intensity of the spots along the azimuthal circle. For an ideal fcc structure, the innermost ring should disappear. The positions of the peaks in the diffraction pattern along the  $\nabla \vec{v}$  direction [ $\vec{v} - (\vec{V} \times \vec{v})$  plane] can be calculated from the form factor of the layered structure. The basis vectors defining the 2D hcp lattice are given by [14]

$$\vec{k}_a = \frac{2\pi}{d} \left( \hat{k}_v - \sqrt{\frac{1}{3}} \hat{k}_e \right), \quad (1)$$

$$\vec{k}_b = \frac{2\pi}{d} \sqrt{\frac{4}{3}} \hat{k}_e, \quad (2)$$

where  $d$  is the lattice constant, and  $\hat{k}_v$  and  $\hat{k}_e$  are unit vectors along the  $\vec{v}$  and  $\nabla \times \vec{v}$  directions, respectively. The peak positions ( $Q_i$ ) correspond to a linear combination of these basis vectors,

$$Q_i = mk_a + nk_b, \quad (3)$$

where  $m$  and  $n = \dots, -2, -1, 0, 1, 2, \dots$ . Therefore, the powder averaged intensity peaks should appear at  $Q_i/Q_0$  ratios,  $1: \sqrt{3}: 2: \sqrt{7}: 3: \sqrt{12}: \dots$ . The peak positions in Figs. 2(a) and 2(b) are in good agreement with those given by Eq. (3), with the first peak ( $Q_0$ ) at  $0.06 \text{ nm}^{-1}$ .

Figure 3 displays the time evolution of the crystallinity, and the rheological parameters  $G'$  and  $G''$  (nonlinear moduli referring to the elastic and viscous parts, respectively) during the oscillatory shearing experiment presented in Fig. 2. The behavior of  $G'$  and  $G''$  indicates the decrease in the dynamic viscosity  $\eta'$  while the elastic part shows only a small variation. The crystallinity was estimated from the height of the first-order peak of the fcc structure ( $q \sim 0.104 \text{ nm}^{-1}$ ), which is taken as a measure of the crystalline ordering within the

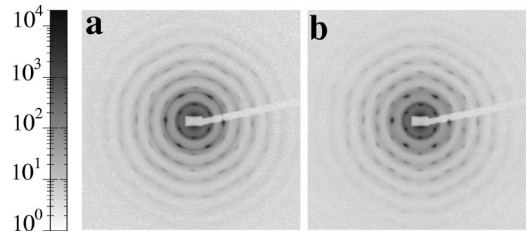


FIG. 4. SAXS patterns of the initially disordered latex suspension after submitting to oscillatory shears of (a)  $\sigma = 200 \text{ Pa}$  and  $f = 4.6 \text{ Hz}$  and (b)  $\sigma = 800 \text{ Pa}$  and  $f = 6.8 \text{ Hz}$ . The low  $\sigma$  and  $f$  pattern shows polycrystalline behavior and at high  $\sigma$  and  $f$  the crystal starts to melt by the high shear.

planes. The behavior is identical if the area of the Bragg peak is followed as a function of time. The peak height  $S(Q_1)$  fluctuated during the ordering process, and then increased abruptly upon the cessation of shear. The full width at half maximum of the peak changed from about  $9 \times 10^{-3} \text{ nm}^{-1}$  to  $8 \times 10^{-3} \text{ nm}^{-1}$  when the oscillatory flow was stopped. The observed fluctuations in the crystallinity are not likely to have been caused by an aliasing effect. The fluctuations are on a much longer time scale than the difference of the sampling frequency (5 Hz) and  $f (= 6.8 \text{ Hz})$ . On the other hand, the evolution of  $G'$  and  $G''$  indicates that the viscosity decreased to the plateau level upon the formation of a layered structure. However, the structure factor evolved more gradually, as the stacking faults are annealed by the oscillatory shear. Therefore, fluctuations in  $S(q)$  signify the defect dynamics resulting from the competition between deformation and annealing. For a given applied stress, the peak deformation increases upon ordering, and this increased deformation can induce more defects. These two competing effects lead to ordering and disordering processes within the layers while slipping past each other. The fast jump upon cessation of flow is controlled by the short time, local-scale particle diffusivity. The particles move back to their equilibrium lattice position. This is also indicated upon reshearing (with the same  $\sigma$  and  $f$ ) the suspension;  $G'$  and  $G''$  remained at their plateau values from the beginning.

Figure 4 depicts the SAXS patterns obtained after oscillatory shears of the same duration but different levels of  $\sigma$  and  $f$ . Low  $\sigma$  and  $f$  are not sufficient to yield a complete alignment and hence the correlation peak of the disordered matrix does not disappear completely. At higher  $\sigma$  levels and  $f$ , the ordering is partly distorted as the crystals begin to shear melt. However, we did not observe a complete transition to disordered close-packed structure even at the highest  $f$  (40 Hz) studied. The best ordering was obtained using a frequency sweep from 1 Hz to 10 Hz, compared to any fixed  $f$  used. The competition between ordering and melting also occurs during steady state conditions, and a coexistence of ordered domains with a disordered random matrix explains the formation of bundles, as will be discussed elsewhere [19].

Coupling a rheometer to SAXS measurements allowed us to monitor the change in microstructure and rheological parameters during the shear-induced ordering of a concentrated

disordered latex suspension. We observed a one-to-one correspondence between the rheological and microstructural changes. In oscillatory shearing, the ordering process is more controlled by the deformation than by the peak stress. Systems with a controlled degree of crystallinity can be made by varying the conditions of the oscillatory flow. Time resolved

rheo-SAXS could be a useful tool to investigate many different soft condensed matter systems.

We thank ESRF for financial support and provision of beam time. J.M. and J.V. wish to acknowledge the Fund for Scientific Research–Flanders (FWO-Vlaanderen) for Grant No. FWO-G.0208.00.NLOT.

- 
- [1] R. A. Lionberger and W. B. Russel, in *Advances in Chemical Physics*, edited by I. Prigogine and S. A. Rice (Wiley, New York, 2000), Vol. 111, p. 399.
- [2] B. J. Ackerson and N. A. Clark, *Phys. Rev. Lett.* **46**, 123 (1981).
- [3] R. L. Hoffmann, *Trans. Soc. Rheol.* **16**, 155 (1972); *J. Colloid Interface Sci.* **46**, 491 (1974).
- [4] H. M. Laun, R. Bung, S. Hess, W. Loose, O. Hess, K. Hahn, E. Hadicke, R. Hingmann, and P. Lindner, *J. Rheol.* **36**, 743 (1992).
- [5] C. Dux and H. Versmold, *Phys. Rev. Lett.* **78**, 1811 (1997); C. Dux, S. Musa, V. Reus, H. Versmold, D. Schwahn, and P. Lindner, *J. Chem. Phys.* **109**, 2556 (1998).
- [6] G. A. McConnell, M. Y. Lin, and A. P. Gast, *Macromolecules* **28**, 6754 (1995).
- [7] F. R. Molino, J.-F. Berret, G. Porte, O. Diat, and P. Lindner, *Eur. Phys. J. B* **3**, 59 (1998).
- [8] K. Mortensen, *J. Phys.: Condens. Matter* **8**, A103 (1996).
- [9] S. Okamoto, K. Saijo, and T. Hashimoto, *Macromolecules* **27**, 3753 (1994).
- [10] J. F. Brady, *Chem. Eng. Sci.* **56**, 2921 (2001).
- [11] A. C. Catherall, J. R. Melrose, and R. C. Ball, *J. Rheol.* **44**, 1 (2000).
- [12] J. Vermant, L. Raynaud, J. Mewis, B. Ernst, and G. G. Fuller, *J. Colloid Interface Sci.* **211**, 221 (1999).
- [13] J. Vermant, *Curr. Opin. Colloid Interface Sci.* **6**, 489 (2001).
- [14] W. Loose and B. J. Ackerson, *J. Chem. Phys.* **101**, 7211 (1994).
- [15] L. Raynaud, B. Ernst, C. Verge, and J. Mewis, *J. Colloid Interface Sci.* **181**, 11 (1996).
- [16] P. Panine and T. Narayanan (unpublished).
- [17] T. Narayanan, O. Diat, and P. Bösecke, *Nucl. Instrum. Methods Phys. Res. A* **177**, 1005 (2001).
- [18] J.-P. Hansen and L. Verlet, *Phys. Rev.* **184**, 151 (1969).
- [19] J. Vermant *et al.* (unpublished).